Wu et al. Biotechnology for Biofuels (2015) 8:78
DOI 10.1186/s13068-015-0262-7

Biotechnology for Biofuels

RESEARCH ARTICLE Open Access

Enzyme activity highlights the importance of the oxidative pentose phosphate pathway in lipid accumulation and growth of *Phaeodactylum tricornutum* under CO_2 concentration

Songcui Wu[1,2†], Aiyou Huang[1†], Baoyu Zhang[1], Li Huan[1,2], Peipei Zhao[1,2], Apeng Lin[1] and Guangce Wang[1*]

Abstract

Background: Rising CO_2 concentration was reported to increase phytoplankton growth rate as well as lipid productivity. This has raised questions regarding the NADPH supply for high lipid synthesis as well as rapid growth of algal cells.

Results: In this study, growth, lipid content, photosynthetic performance, the activity, and expression of key enzymes in Calvin cycle and oxidative pentose phosphate pathway (OPPP) were analyzed in the marine diatom *Phaeodactylum tricornutum* under three different CO_2 concentrations (low CO_2 (0.015 %), mid CO_2 (atmospheric, 0.035 %) and high CO_2 (0.15 %)). Both the growth rate and lipid content of *P. tricornutum* increased significantly under the high CO_2 concentration. Enzyme activity and mRNA expression of three Calvin cycle-related enzymes (Rubisco, 3-phosphoglyceric phosphokinase (PGK), phosphoribulokinase (PRK)) were also increased under high CO_2 cultivation, which suggested the enhancement of Calvin cycle activity. This may account for the observed rapid growth rate. In addition, high activity and mRNA expression of G6PDH and 6PGDH, which produce NADPH through OPPP, were observed in high CO_2 cultured cells. These results indicate OPPP was enhanced and might play an important role in lipid synthesis under high CO_2 concentration.

Conclusions: The oxidative pentose phosphate pathway may participate in the lipid accumulation in rapid-growth *P. tricornutum* cells in high CO_2 concentration.

Keywords: CO_2, Lipids, Enzyme activity, Oxidative pentose phosphate pathway, *Phaeodactylum tricornutum*

Background

As a result of increased industrialization and human activities, global carbon dioxide (CO_2) emission has increased dramatically and induces seawater acidification, which affects the growth and photosynthesis of marine phytoplankton [1]. Photosynthetic CO_2 fixation by phytoplankton (e.g., eukaryotic microalga) mainly depends upon Calvin cycle, and ribulose-1, 5-bisphosphate carboxylase/oxygenase (Rubisco) catalyzes the initial step of CO_2 fixing. The response of photosynthesis, metabolite including the Calvin cycle enzymes (especially Rubisco), and growth to elevated CO_2 have been well studied in higher plants. It was shown that short-term CO_2 elevating generally accelerates carbon fixation and leads to an increase of Rubisco activity followed by an enhancement of growth in C_3 plants [2–6]. Yet, in the long-term, the photosynthesis decreased with increasing CO_2, which is typically accompanied by a decline in the amount and activity of Rubisco and other enzymes in the Calvin cycle and a decrease of growth rates. Compared to high plants, the impacts of elevated CO_2 concentration on microalgae and their response to CO_2 levels, especially Calvin cycle enzyme (including Rubisco) activity and amount, have been learned much less extent and attentions mainly paid to photosynthesis and algal growth. Only in the study of *Euglena gracilis* Z, Nakano et al. focused on Rubisco and found Rubisco activity was higher in high CO_2 conditions [7]. Whereas, elevated CO_2 concentration

* Correspondence: gcwang@qdio.ac.cn
†Equal contributors
[1]Key Laboratory of Experimental Marine Biology, Institute of Oceanology, Chinese Academy of Sciences, Nanhai Road 7, Qingdao 266071, China
Full list of author information is available at the end of the article

increased the efficiency of photosynthetic carbon fixation and growth of phytoplankton was gradually known as general phenomenon [8, 9]. Kim et al. [10] reported that the growth of *Skeletonema costatum* enhanced at higher concentrations of CO_2. Tortell et al. [11] also found that rising CO_2 can enhance *Chaetoceros* spp. growth. In addition, various studies have shown that rising CO_2 concentration increases lipid productivity as well as phytoplankton growth rate, such as in *Phaeodactylum tricornutum* [12], *Nannochloropsis oculata* [13], and *Chlorella vulgaris* [14], high levels of CO_2 concentration enhanced both biomass production and lipid content, thus shedding light on the potential for biodiesel production from microalgae. To select microalgae for obtaining a higher lipid productivity, even higher concentrations of CO_2 (10 % CO_2 and flue gas) were used to cultivate *Botryococcus braunii* and *Scenedesmus* sp. [15]. At present, about 60 species of microalgae have been well domesticated with high concentration of CO_2 for producing large biomass and achieving high biofuel yields [16]. However, most previous studies have only focused on microalgal growth rate, lipid content, and tolerance to high levels of CO_2 [17–20]. Little effort has been directed toward the analysis of the mechanism involved in lipid accumulation in microalgae and their simultaneous rapid growth rate.

Microalgal lipids, as a source of biofuel, are usually derived from long-chain fatty acids, which require NADPH for synthesis [21, 22]. For example, to produce an 18-carbon fatty acid, 16 NADPH molecules are required as electron donors. Therefore, enhanced lipid accumulation will surely increase metabolic demand in microalgae for NADPH. Microalgae have been demonstrated to grow rapidly in high CO_2 concentrations. This suggests that quantity of NADPH, which is supplied by the light reaction, is required for photosynthetic carbon fixation which supplies substrates and energy for the synthesis of major constituents (proteins, nucleic acids, and carbohydrates) essential for algal growth. For effective CO_2 fixation, ATP and NADPH produced by photosynthetic light reactions must be maintained at a molar ratio of 3:2 [23]. Once a large number of NADPH molecules are consumed, the ratio will be disrupted leading to a reduction in carbon fixation activity. An important question therefore remains about how NADPH is supplied for high fatty acid synthesis as well as rapid growth of algal cells cultured under high CO_2 concentration. It is more likely that another pathway may contribute to providing this reductant.

In the present study, we evaluated the lipid content in the diatom *P. tricornutum* which was cultivated in three different CO_2 conditions (0.015 %, atmospheric, and 0.15 %). Furthermore, we measured the activity of seven key enzymes and mRNA expression in *P. tricornutum* to explore the mechanism of rapid growth and the simultaneous increase in lipid accumulation in high-CO_2 cultured algal cells. Our research showed that the pentose phosphate pathway may be incorporated in maintaining the NADPH supply under high CO_2 concentrations.

Results

Algal growth, pH changes, and photosynthetic performance under low, mid, and high CO_2 concentrations

When grown under low, mid, and high CO_2 concentrations, the growth rate of *P. tricornutum* showed significant differences among the groups. The highest growth rate occurred under high CO_2 concentration and was 0.20 at the beginning of treatment and 0.70 on the seventh day at the optical density (OD) of 730 nm, followed by mid CO_2 concentration, and was 0.20 at the beginning of treatment and 0.41 on the seventh day at $OD_{730\ nm}$. No significant growth was observed in the low-CO_2 cultured alga (Fig. 1a). This indicated that when nutrients were sufficient, the carbon source performs as the limiting factor which affected algal growth.

Figure 1b shows that the medium pH had a significant increase on day 1 under both mid-CO_2 (from 8.83 to 9.41) and low-CO_2 (from 8.83 to 9.45) conditions, and from day 2 to 7, the pH of mid-CO_2 and low-CO_2 cultures gradually increased, whereas the pH of algal culture bubbled with high level of CO_2 strongly decreased on day 1 (from 8.83 to 7.07) and then gradually increased from 7.07 to 8.32. Faster growth and greater carbon fixation were observed in high-CO_2 cultured *P. tricornutum* under the low pH and high CO_2 condition. The consumption of NO_3^- during algal rapid growth may cause the increase of culture pH from day 2 to 7 under high CO_2 concentration, and this increase of pH might correlate with algal growth rate and carbon fixation efficiency. Compared with high-CO_2 culture, both mid- and low-CO_2 cultures had an increase of culture pH values associated with a relative slow growth after bubbled with mid and low levels of CO_2 from day 2 to 7.

As shown in Fig. 1c, d, both high-CO_2 and mid-CO_2 cells obtained high values of maximal photosynthesis system II (PSII) quantum yield (F_v/F_m) and effective PSII quantum yield (YII) during cultivation, and they all firstly represented a significant increase of F_v/F_m and Y (II) values and then gradually decreased. The high-CO_2 cells consistently had the highest F_v/F_m and Y (II) values, followed by mid carbon cultured alga. Whereas, low CO_2 cultivated alga had the lowest F_v/F_m and Y (II) values, which obviously decreased during cultivation. This suggested that the response to CO_2 concentration in algal cells was also reflected in the changes in algal photosynthesis.

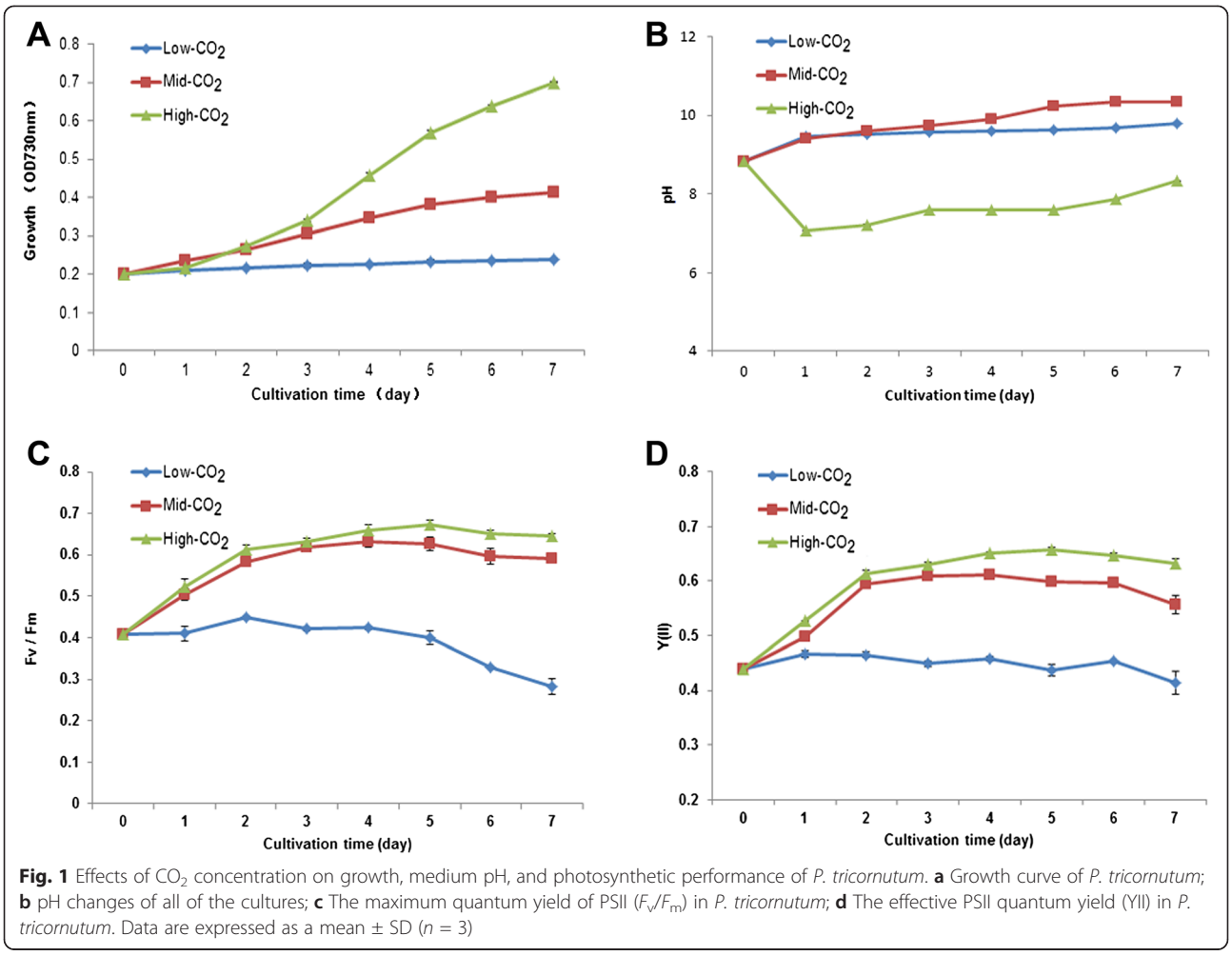

Fig. 1 Effects of CO_2 concentration on growth, medium pH, and photosynthetic performance of *P. tricornutum*. **a** Growth curve of *P. tricornutum*; **b** pH changes of all of the cultures; **c** The maximum quantum yield of PSII (F_v/F_m) in *P. tricornutum*; **d** The effective PSII quantum yield (YII) in *P. tricornutum*. Data are expressed as a mean ± SD (n = 3)

Lipid, fatty acid composition, total water-soluble proteins, chlorophyll *a* + *c* content and RNA concentration in algal cells measured under different CO_2 concentrations

As described above, the concentration of CO_2 had significant effects on *P. tricornutum* growth. To investigate the influence of CO_2 concentrations on intracellular substances, we determined the lipid, total water-soluble proteins, and chlorophyll *a* + *c* content in *P. tricornutum* treated with different CO_2 concentrations. Table 1 shows that when grown under the high CO_2 condition, *P. tricornutum* had the highest lipid content (53.71 ± 2.41 %, *w*/*w*, % of dry cell weight (DCW)), followed by mid CO_2 cultivated cells of 35.87 ± 1.72 %, and low CO_2 cultured *P. tricornutum* had the lowest lipid content of 33.13 ± 1.21 %. As shown in Table 2, in low- and mid-CO_2 cultured cells, 7.41 % (% of DCW) and 8.72 % (% of DCW) are longer-chain fatty acids (≥20C), respectively. Whereas, in high-CO_2 cultured cells, the longer-chain fatty acids (≥20C) account in 16.41 % of dry cell weight. It was represented that a significant increase of longer-chain fatty acids content in high-CO_2 cultured cells, compared to low- and mid-CO_2 cultured cells. These results suggested

Table 1 Dry weight and intracellular substances contents in three different CO_2 concentrations cultivated *P. tricornutum* cells. Intracellular substances involved total water-soluble protein, lipids, chlorophyll a + c and RNA concentration. Data are expressed as a mean ± SD (n = 3)

CO_2 concentration	Low-CO_2 (0.015 %)	Mid-CO_2 (0.035 %)	High-CO_2 (0.150 %)
Culture dry weight (g L^{-1})	0.083	0.109	0.245
Lipid content (*w*/*w*, % of DCW)	33.13 ± 1.2	35.87 ± 1.7	53.71 ± 2.4
Chlorophyll *a* + *c* concentration (mmol g^{-1} FW)	2.52 ± 0.084	3.73 ± 0.030	3.28 ± 0.084
RNA concentration (μg g^{-1} FW)	378.10 ± 10.42	715.40 ± 15.45	562.39 ± 33.51
Total water-soluble protein production (mg g^{-1} FW)	7.63 ± 0.03	12.76 ± 0.04	16.29 ± 0.02

Table 2 Fatty acid compositions of *P. tricornutum* under different CO_2 concentration cultivation (w/w, % of DCW)

Fatty acids	Low-CO_2 (%)	Mid-CO_2 (%)	High-CO_2 (%)
14:0	3.52	3.82	5.10
16:0	4.65	6.03	8.67
16:1ω7	6.61	8.28	12.25
16:2ω4	1.29	1.62	1.95
16:3ω4	2.01	2.57	3.20
16:4ω1	0.29	0.46	0.43
18:0	3.85	3.49	4.87
18:2ω6	0.99	0.80	0.83
20:5ω3	5.17	6.80	11.58
22:0	0.27	0.16	0.78
22:4ω7	0.44	0.22	0.64
22:5ω3	0.26	0.34	0.79
24:0	1.27	1.21	2.62
Total 14~18C	25.72	27.06	37.30
Total 20~24C	7.41	8.72	16.41

that the high-CO_2 cultured cells need much more cytosolic-generated reductant for lipids or longer-chain fatty acid synthesis.

Table 1 exhibits the maximum water-soluble protein yield 16.29 ± 0.02 mg g^{-1}FW in *P. tricornutum* also occurred in the high CO_2 cultivated cells, while the mid-CO_2, and low-CO_2 cells had relatively lower soluble protein contents of 12.76 ± 0.04 and 7.63 ± 0.03 mg g^{-1} fresh weight (FW), respectively. Although high-CO_2 *P. tricornutum* cells had high lipid and water-soluble protein contents, the concentration of chlorophyll *a* + *c* and RNA were lower than those in mid CO_2 cultured cells (Table 1). Low-CO_2 cultured cells had the lowest yield of intracellular substances, which may have been due to the limiting of carbon source.

Assays of the change in enzyme activities

P. tricornutum maintained in high CO_2 concentration had the highest growth rate among the three experimental groups (Fig. 1). To investigate the mechanism underlying the different growth rates due to CO_2 concentration, the activities of key enzymes in the Calvin cycle, including Rubisco, 3-phosphoglyceric phosphokinase (PGK), and phosphoribulokinase (PRK) were analyzed. As shown in Fig. 2, these enzymes showed maximum activity in *P. tricornutum* under the high CO_2 concentration, followed by mid-CO_2 cultured cells, which were slightly higher than low-CO_2 cultured cells, but no significant difference was observed in the activity of PRK between mid-CO_2 and low-CO_2 cultured cells ($P > 0.05$). These results suggest that the activity of the Calvin cycle was enhanced under high CO_2 cultivation, which was well matched with the high growth rate and photosynthetic performance of *P. tricornutum* in the high-CO_2 concentration.

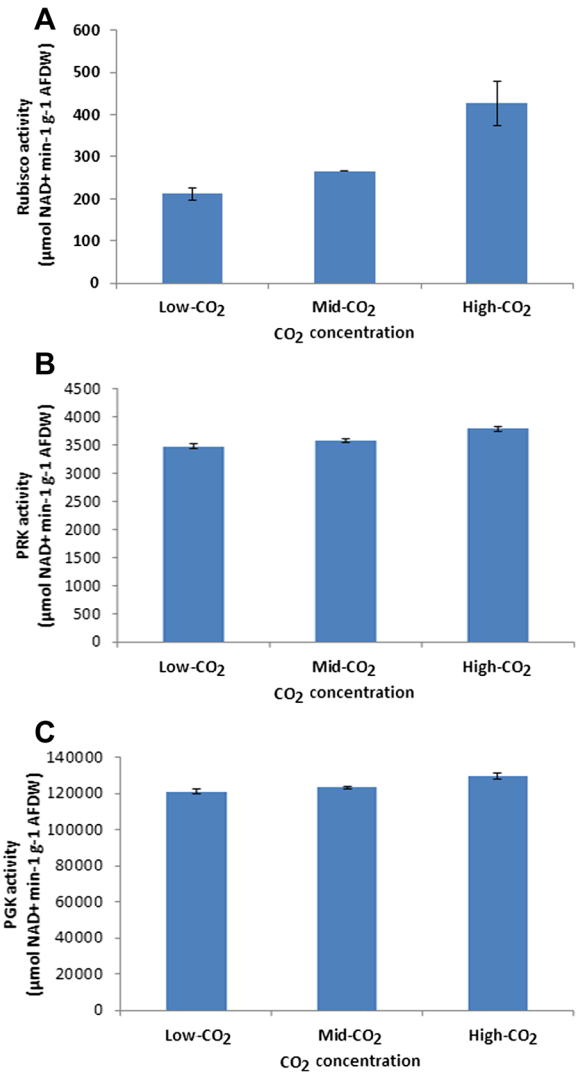

Fig. 2 Changes of Calvin cycle-related enzymes' activities in *P. tricornutum* cells responded to different CO_2 concentrations. **a** The activity of Rubisco in *P. tricornutum*; **b** The activity of PRK in P. tricornutum; **c** The activity of PGK in *P. tricornutum*. Data are expressed as a mean ± SD ($n = 3$)

In addition, alga cells grown under the high CO_2 concentration had a maximum yield of lipids (Table 1). This prompted us to investigate probable pathways which supplied NADPH for lipid synthesis, as NADPH is essential for elongation of fatty acids. To the best of our knowledge, in the photosynthetic cells of plants, de novo biosynthesis of 16-carbon and 18-carbon fatty acids occurs in the chloroplast, where NADPH is produced via the light reactions of photosynthesis. The 16-carbon fatty acids (e.g., palmitate) are elongated to yield the 20-carbon and even longer-chain fatty acids in the cytosol, so these elongation steps are the only ones that require cytosolic-generated reductant [24].

The oxidative pentose phosphate pathway (OPPP) is the major resource of NADPH in the cytoplasm. To better understand the carbon flux and reductant source for lipid synthesis in *P. tricornutum* cells under three different CO_2 concentrations, the activities of G6PDH and 6PGDH, two key enzymes in the OPPP, were evaluated. Figure 3 shows the activities of G6PDH and 6PGDH, and these results showed that G6PDH and 6PGDH activities were highest under high-CO_2 cultivation, while algal cells maintained in mid- and low-CO_2 showed lower and lowest activity, respectively. These findings indicate that the activity of the OPPP was enhanced in cells under high-CO_2 cultivation and may have supplied NADPH for lengthening the fatty acids chain.

As the OPPP is not the sole producer of NADPH, to verify whether the other sources for NADPH could contribute to cytosolic fatty acids elongation, two tricarboxylic acid (TCA) cycle enzymes activity were detected. Figure 4 shows that no significant differences were observed in the activity of MDH of three different CO_2 concentration cultured *P. tricornutum* cells. Whereas, the activity of α-ketoglutarate dehydrogenase (α-KGDH) was peaked in high-CO_2 cultivated *P. tricornutum* cells, followed by mid-CO_2 cells, and the low-CO_2 cultivated cells had the lowest α-KGDH activity. As α-KGDH is the rate-determining enzyme of the TCA cycle [25], the activity of α-KGDH was positively correlated with TCA cycle activity. High α-KGDH activity indicated a general enhancement of the TCA cycle under high CO_2 concentration.

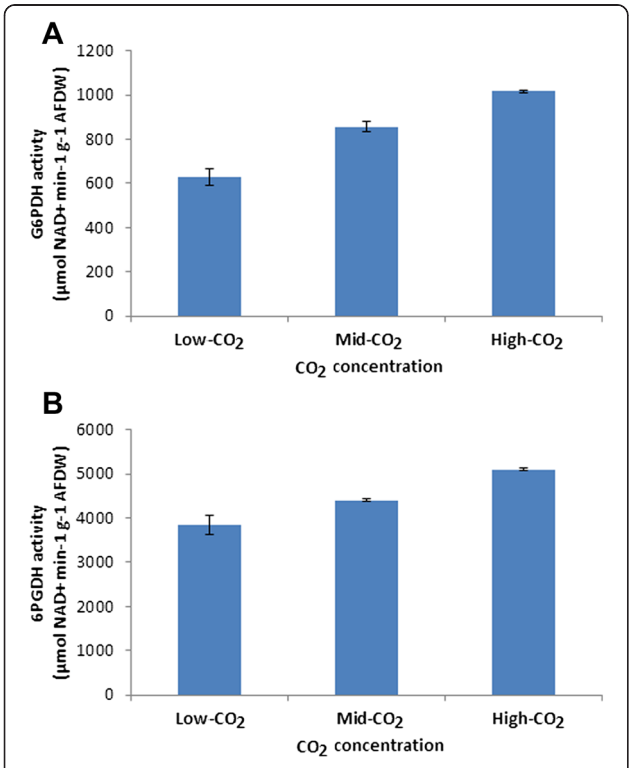

Fig. 3 G6PDH and 6PGDH activities in *P. tricornutum* maintained with three different CO_2 concentrations. Both G6PDH and 6PGDH had relatively high activities in high-CO_2 cultivated *P. tricornutum* cells. **a** The activity of G6PDH in *P. tricornutum*; **b** The activity of 6PGDH in *P. tricornutum*. Data are expressed as a mean ± SD (n = 3)

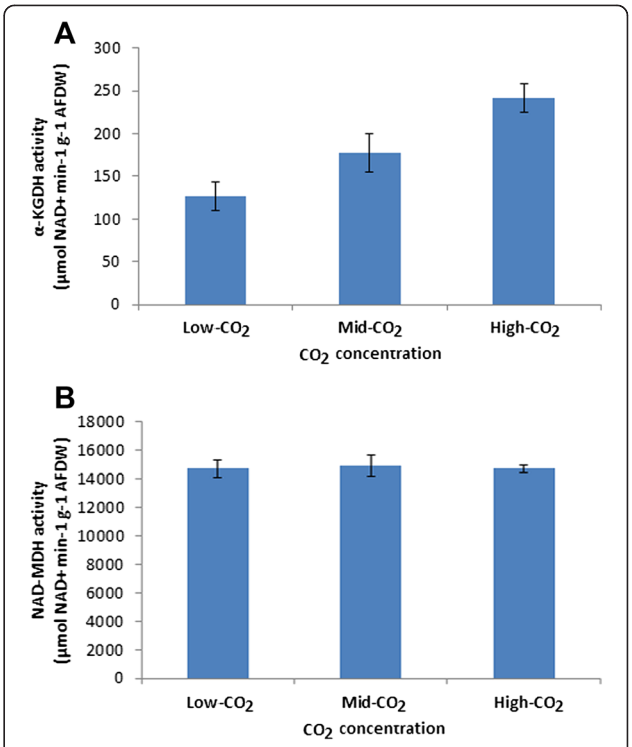

Fig. 4 The activities of two TCA cycle enzymes in *P. tricornutum* cultured with different CO_2 concentrations. **a** The activity of α-KGDH; **b** The activity of MDH. Data are expressed as a mean ± SD (n = 3)

Analysis of enzyme mRNA expression measured by qPCR

The results of real-time PCR showed that under high CO_2 concentration, *P. tricornutum* had the highest relative expression level of Rubisco, PRK, PGK, G6PDH, and 6PGDH among the three treatments (Figs. 5 and 6). The expressions of Rubisco, PGK, and G6PDH in mid-CO_2 cultivated *P. tricornutum* cells were higher than those of the low-CO_2 cultured cells, but the expression of PRK and 6PGDH in mid -CO_2 cultivated *P. tricornutum* was not significantly different to that found in low-CO_2 cultured cells ($P > 0.05$) The mRNA expression level of these enzymes was consistent with the results of enzyme activity, which indicated that *P. tricornutum* under high CO_2 cultivation not only had high enzyme activities but also high mRNA content. Higher enzyme activities and mRNA expression levels of Rubisco, PGK, and PRK suggested that, in Calvin cycle, the CO_2 fixation, carbon reduction, and ribulose-1,5-bisphosphate (RuBP) regeneration were enhanced; in other words, the

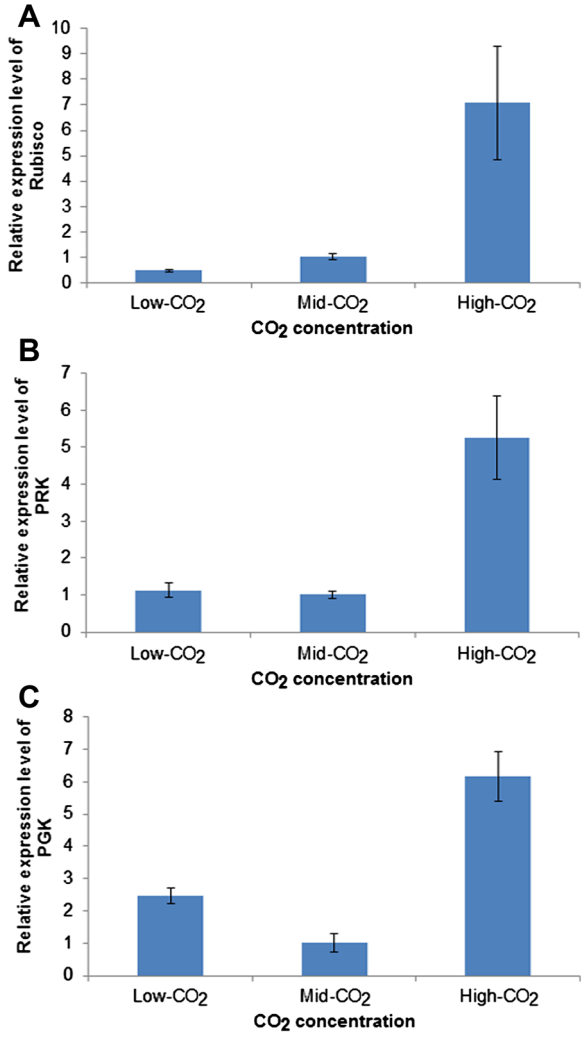

Fig. 5 Three enzymes' mRNA expression in different CO_2 concentrations cultured *P. tricornutum* cells measured by qPCR. **a** Rubisco expression in *P. tricornutum*; **b** PRK expression in *P. tricornutum*; **c** PGK expression in *P. tricornutum*. Data are expressed as a mean ± SD ($n = 3$)

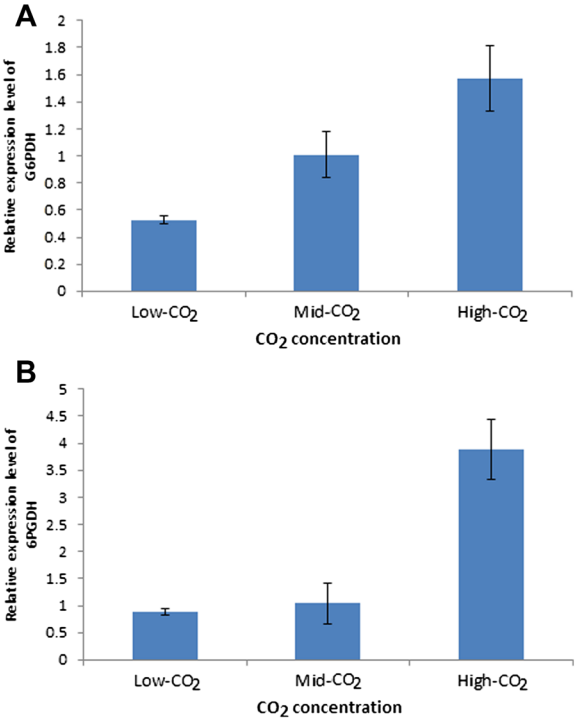

Fig. 6 The expressions of G6PDH and 6PGDH in *P. tricornutum* cultured with different CO_2 concentration. **a** The relative expression level of G6PDH; **b** The relative expression level of 6PGDH. Data are expressed as a mean ± SD ($n = 3$)

carbon fixation efficiency of Calvin cycle elevated and the production of carbon skeleton for biosynthesis increased. These might positively correlate with rapid growth of *P. tricornutum* under high CO_2 concentration.

Discussion

As described in Fig. 1, *P. tricornutum* can tolerate relatively high levels of CO_2 and has a rapid growth rate when cultivated in high CO_2 concentration, which was consistent with the finding that rising CO_2 concentration increased phytoplankton growth rate [1, 8, 9, 12, 26]. Moreover, Rubisco activity and mRNA expression were increased (Figs. 2 and 5) under high CO_2 concentration. As the rate-limiting and key regulatory enzyme of the Calvin cycle, the level of Rubisco monitors the carbon flux through this pathway [27]. In addition to high Rubisco activity, the activities of PRK and PGK were high in high CO_2 concentration cultured cells and significantly higher than Rubisco activity. Rubisco acts as a CO_2 receptor and takes part in the carbon fixation stage of the Calvin cycle, and PGK participates in the reduction stage of the Calvin cycle, whereas PRK is incorporated in the regeneration phase in the Calvin cycle; high activities of Rubisco, PGK, and PRK in high CO_2 cultured cells indicated that the Calvin cycle activity was enhanced and was operating effectively in algal cells under high CO_2 cultivation. This may account for the rapid growth rate observed. However, when *P. tricornutum* was grown under low CO_2 concentration, the activities of the Calvin cycle-related enzymes were weaker, which suggested that substrates and energy required for algal growth were deficient. This might be the major reason why no significant growth under the low CO_2 concentration of algal cells was observed. These results indicated elevated CO_2 concentration provided plenty of carbon resource for photosynthetic carbon fixation and then induced an enhancement of algal photosynthetic carbon fixation and growth rate which were consistent with numerous previous studies that higher levels of CO_2 support higher growth rates.

As expected, a significant increase in lipid content was also found in the high CO_2 cultivated rapid-growth *P. tricornutum* cells. As we know, microalgal lipid production typically begins at the onset of nitrogen depletion as the

C/N ratio (carbon to nitrogen ratio) in algal cells increased, which lead to most of the fixed carbon divert into nitrogen deficient compounds such as lipids [28]. In this research, *P. tricornutum* were maintained in nitrogen repletion cultures, which might not trigger lipid accumulation. Yet we observed 1.5-fold increase of lipid content in high-CO_2 cultured cells, compared to mid-CO_2 cultured cells. We thought that maybe because of a higher C/N ratio in algal cells that caused by high CO_2 concentration. This is supported by the conclusion that the elemental stoichiometry (carbon to nitrogen ratio) was raised under high CO_2 conditions in both nitrogen limited and nitrogen replete conditions in *P. tricornutum* according to Li et al. [29].

Lipids, especially triacylglycerol (TAG), primarily serve as a storage form of carbon and energy in algal cells [30], which require numerous NADPH molecules for biosynthesis in the cytoplasm. During rapid growth of algal cells, ATP and NADPH generated by the light reaction are mainly supplied for the maintenance of algal growth. Therefore, under high CO_2 cultivation, the key problem in the rapid growth of algal cells is how the additional NADPH required for lipid synthesis comes from. NADPH can be primarily generated from the OPPP or TCA cycle. The first two steps of the OPPP, catalyzed by G6PDH and 6PGDH respectively, are the major source of NADPH. As shown in Fig. 6, with a high level of CO_2 concentration, enhanced activity and mRNA expression of G6PDH and 6PGDH were observed, except for increased lipid accumulation, which indicated that OPPP activity was enhanced. In a study of *Chlorella*, Xiong et al. [31] found that NADPH supplied through OPPP increased under nitrogen limited condition when lipid synthesis increased, and they speculated that NADPH from the mitochondrial TCA cycle was difficult to be trapped for lipid metabolism in the cytoplasm. The enhancement of TCA cycle might contribute to two possibilities: (i) to provide ATP for lipid synthesis; (ii) to produce quantity of intermediates (e.g., malic acid) to offer substrate or carbon skeleton for fatty acid synthesis [32]. Thus, G6PDH together with 6PGDH that are of great importance in the synthesis of the reductant NADPH through the OPPP [33], may play an important role in elongation of fatty acids under high CO_2 concentration.

Conclusions

In this study, growth, lipid content, photosynthetic performance, the activity, and expression of key enzymes in Calvin cycle and OPPP were analyzed in the marine diatom *P. tricornutum* under three different CO_2 concentrations. Both the growth rate and lipid content of *P. tricornutum* increased significantly under the high CO_2 concentration. Enzyme activity and mRNA expression of three Calvin cycle-related enzymes (Rubisco, PGK, PRK) were also increased under high CO_2 cultivation, which suggested the enhancement of the Calvin cycle activity. This may account for the observed rapid growth rate. In addition, high activity and mRNA expression of G6PDH and 6PGDH, which produce NADPH through OPPP, were observed in high CO_2 cultured cells. These results indicate OPPP was enhanced and might play an important role in elongation of fatty acids or lipid synthesis under high CO_2 concentration.

Methods

Alga strain cultivation

P. tricornutum was screened from the East China Sea and confirmed unialgal as previously described by Wu et al. [34]. The alga strain was cultivated in sterilized carbon source deprived artificial seawater enriched with f/2-Si medium [35] and grown at 20 ± 1 °C under a constant light intensity of 100 μmol m^{-2} s^{-1} with a 14:10 h light-dark (L/D) cycle.

CO_2 treatment

The alga culture was maintained with aeration and cultivated in 2-L flasks containing 1.5-L medium. Three different CO_2 concentrations in the bubbling aeration system were tested: low CO_2 (0.015 %), mid CO_2 (atmospheric, 0.035 %), and high CO_2 (0.15 %). The handheld indoor air quality testing detector Telaire 7001 CO_2 Monitor (USA), which can be able to display CO_2 readings in less than 30 s, was used to measure CO_2 concentration in this study. Each treatment included three replicates. The pH of algal culture bubbled with different CO_2 concentration was daily measured using a Switzerland Mettler Toledo Delta 320 pH meter.

Growth and photosynthetic determination

Algal growth was measured daily by cell number and the OD value at the optical wavelength for *P. tricornutum* (730 nm) using a spectrophotometer (UV-1800). A hemocytometer was used to count algal cells.

To investigate the photosynthetic performance of *P. tricornutum* in response to CO_2 concentration, the chlorophyll fluorescence of PSII was measured by a Dual-PAM-100 fluorometer (Heinz Walz, Effeltrich, Germany) which was conducted with a PC using the WinControl software (Heinz Walz). Two parameters, the maximum quantum yield of PSII (F_v/F_m) and the effective PSII quantum yield (YII), were evaluated using the pulse-amplitude modulated method as described by Lin et al. [36] with some modifications. To ensure the consistency of cell density for PAM fluorescence measurement, the growing algal samples were adjusted to 0.6 at $OD_{730\ nm}$ before detected. The minimum fluorescence (F_0) and maximum fluorescence (F_m) were determined after the samples were incubated in darkness for 5 min.

Variable fluorescence (F_v) was calculated according to formula $F_v = F_m - F_0$. The maximal PSII quantum yield was calculated as F_v/F_m. The effective quantum yield of PSII (Y (II)) was calculated as $(F'_m - F)/F'_m$, where F'_m was the maximal fluorescence detected under photosynthetic active radiation (PAR) of 58 μmol m^{-2} s^{-1} and F is the real-time fluorescence yield under illumination.

Lipid analysis

Algal cultures were harvested after 7-day cultivation by centrifugation at 5000*g*, and the algal cells were quickly frozen in liquid nitrogen. A freeze dryer was used to dry the frozen algal cells. Lipids were extracted from 50 mg dryness algal powder using a modified chloroform-methanol system as described by Bligh and Dyer [37]. Crude samples were dried with N_2 flow until a constant weight was obtained. Gravimetric means, a conventional lipid quantification method, was used for total lipid analysis. The fatty acid compositions of different CO_2 concentration cultivated *P. tricornutum* were determined by gas chromatography [38].

Enzyme assays

Harvested algal cells were washed twice with 0.01 M PBS buffer (pH 7.4) and were ground into fine powder using a pre-chilled mortar and pestle with liquid N_2. Crude enzyme extracts were prepared from the algal powder in three times the volume of ice-cold extraction buffer. Enzyme activities were determined spectrophotometrically using a UV-1800 spectrophotometer by measuring at 340 nm in total volumes of 0.4 mL and in triplicate. The change in absorbance was recorded for 5 min. Results were expressed as μmol NAD (P) H oxidation or NAD (P) $^+$ reduction min $^{-1}$ g $^{-1}$ AFDW, as we had standardized the correlation between fresh weight and ash-free dry weight of different CO_2 cultured *P. tricornutum*. The compositions of the extract and assay medium for the respective enzymes are detailed below. All chemicals and enzymes used for enzyme assays were purchased from Sigma-Aldrich (Sigma-Aldrich Co. LLC., USA).

Rubisco (ribulose-1, 5-bisphosphate carboxylase/oxygenase), which controls the initial step in photosynthetic carbon fixation via the Calvin cycle, is one of the most abundant proteins in both higher plants and algae [39]. The carboxylase activity of Rubisco relative to photosynthetic rates has been reported in many previous studies of macroalgae and microalgae [27]. Rubisco (EC 4.1.1.39) activity was measured using a modification of the basic procedure according to Gerard and Driscoll [27]. 300 μL of chilled extraction buffer (40 mM Tris-HC1, 0.25 mM EDTA, 10 mM $MgCl_2$, 5 mM glutathione, at pH 7.6) was added per 100-mg fresh algal powder. The mixture was stirred for 2 min to homogeneity, and centrifuged at 13,000*g* for 10 min. The supernatants were incubated on ice for further enzyme assays. The reaction mixture contained 0.1 M Tris-HCl (pH 7.8), 0.2 mM $NaHCO_3$, 12 mM $MgCl_2$, 5 mM NADH, 50 mM ATP, 50 mM phosphocreatine, 160 units per milliliter of creatine phosphokinase (EC 2.7.3.2), and PGK (EC 2.7.2.3), and 25 mM RuBP was added to initiate the reaction.

For measurement of PRK (EC 2.7.1.19) and PGK activities in crude extracts, the method described by Rao and Terry [40] was used. Frozen fresh algal cells were extracted in three times the volume of extraction buffer (100 mM Hepes-NaOH (pH 8.0), 10 mM $MgCl_2$, 0.4 mM EDTA, 1 % polyvinypyrrolidone, 100 mM Na-ascorbate, 0.1 % BSA at 0–4 °C) and then stirred for 2 min with a vortex at a maximum speed. Crude homogenates were then centrifuged at 13,000*g* for 10 min. The supernatants were prepared for further assays. For the assay of PRK, pre-chilled 30 mM Hepes-NaOH (pH 8.0), containing 10 mM $MgCl_2$, 5 mM DL-Dithiothreitol (DTT), 2 mM ATP, 2 mM phosphoenolpyruvic acid, 0.4 mM ribose-5-phosphate, 0.3 mM NADH, 2 units per mL of ribose-5-phosphate isomerase (EC 5.3.1.6), lactic dehydrogenase (EC 1.1.1.27), and pyruvate kinase (EC 2.7.1.40) was used as the assay media; the reaction was initiated by adding the algal extract. The activity of PGK (EC 2.7.2.3) was assayed in 30 mM Hepes-KOH (pH 7.8), 5 mM $MgCl_2$, 1 mM NaF, 1 mM KH_2PO_4, 5 mM DTT, 2 mM ATP, 4 mM phosphoglycerate, 0.3 mM NADH, and 4 units per mL of NAD-glyceraldehyde-3-phosphate dehydrogenase (EC 1.2.1.12) and triose phosphate isomerase (EC 5.3.1.1); the reaction was initiated by adding ATP.

The oxidation pentose phosphate pathway is the major resource of cytosolic-generated NADPH, which is catalyzed by G6PDH and 6PGDH. G6PDH, the rate-limiting and key regulatory enzyme of the OPPP, controls the flow of carbon through this pathway and produces reductant to meet the cellular needs for reductive biosynthesis. To determine the activities of G6PDH (EC 1.1.1.49) and 6PGDH (EC 1.1.1.44), the method described by Fahrendorf et al. [41] was used with some modifications. Algal cells prepared as described above were extracted in 50 mM Tris-HC1 pH 8.0, 300 mM NaC1, 0.1 mM benzamidine, and 0.1 mM phenylmethylsulfonyl fluoride (PMSF). G6PDH activity was measured in a continuous assay at 30 °C, including 0.1 M Tris-HC1 pH 8.0, 0.4 mM $NADP^+$, and 3 mM glucose-6-phosphate. 6PGDH activity was measured at 30 °C in 0.1 M Hepes pH 7.5, 0.4 mM $NADP^+$, and 3 mM 6-phosphogluconate. Reactions were started by the addition of algal extracts. Reduction of $NADP^+$ at 340 nm was used to monitor G6PDH and 6PGDH activities.

TCA cycle is another major resource of NADPH, via isocitrate dehydrogenase. To verify whether this process contributes reductant to fatty acid elongation, the activity of two TCA cycle enzymes, α-KGDH and MDH was

measured following the method as described by Peng L and Shimizu K [42]. Algal cells were extracted in 100 mM Tris-HCl (pH 7.0) containing 20 mM KCl, 5 mM MnSO4, 2 mM DTT, and 0.1 mM EDTA. The assay conditions were as follows: α-KGDH 0.2 M phosphate buffer (pH 7.2), 1 mM CoASH, 0.1 M cysteine-HCl (pH 7.2), 10 mM NAD+ (pH 7.2), 3 mM a-ketoglutarate. Malate dehydrogenase, 0.1 M Tris-HCl (pH 8.8), 0.1 mM sodium malate, 10 mM NAD+, and reactions were started by the addition of algal extracts.

Real-time PCR analysis

Total RNA was extracted from frozen algal powder using the Plant RNA kit (OMEGA, Norcross, USA) following the manufacturer's instructions which included the first step of genomic DNA digestion. The concentrations of RNA extracts were measured using a NanoDrop 1000 Spectrophotometer (Thermo, Wilmington, Delaware, USA).

For single strand cDNA synthesis, the PrimeScript RT regent Kit with gDNA Eraser (TaKaRa Biotech Co., Dalian, China) was used to perform the reverse transcription reaction according to the user's manual. In this protocol, further genomic DNA removal was performed to purify the RNA extracts. All tests were performed on ice. PCR was performed to confirm the absence of genomic DNA contamination.

Real-time PCR was performed with the cDNA template from the reverse transcription reaction and five pairs of specific primers (Table 3). Primers were designed based on the alignment of the deduced amino-acid sequences, which were obtained from the National Center for Biotechnology Information (NCBI) web site (http://www.ncbi.nlm.nih.gov/blast), using the Primer Premier 5.0 software. Levels of specific mRNA transcripts were quantified by the Bio-Rad iQ5 Multicolor Real-Time PCR Reaction system (Bio-Rad, Hercules, CA, USA). The real-time PCR amplifications were performed with the reagents from the Fast Essential DNA Green Master (Roche, Germany). The cycling parameters for real-time PCR were 95 °C for 10 min (denaturation), followed by 40 cycles at 94 °C for 10 s (denaturation), 58 °C for 20 s (primer annealing), and (c) 72 °C for 10 s (elongation). To ensure only the single specific DNA fragment was amplified, melting curve analyses were performed on all PCR products. Triplicate qPCRs were performed for each sample. Data derived from the PCR program were analyzed with the Bio-Rad optical system software.

Chlorophyll estimations

For *P. tricornutum*, the chlorophyll *a* and *c*1 + *c*2 content was estimated by a 90 % acetone extraction system. Fifty-milligram fresh algal powder ground from frozen algal cells in liquid N_2 was added in 5 mL 90 % acetone and thereafter read the fluorescence emission of the centrifuged extracts at 664 and 630 nm which were obtained as described by Jeffrey and Humphrey [43].

Total water-soluble proteins preparations

P. tricornutum water-soluble proteins were prepared using the method according to Wang et al. [44] with some modifications. Algal water-soluble proteins were extracted in fivefold volume of pre-chilled extract buffer, containing 50 mM Tris-HCl buffer (pH 8.0), 3 mMDTT, 5 mM $MgCl_2$, 10 % glycerol, 0.5 % polyvinylpyrrolidone (PVP), 5 mM Na_2-EDTA, 1 mM PMSF, 5 mM benzimidin, 5 mM Acoproicand, 1 % (*v*/*v*) plant protease inhibitor cocktail (Sigma). Crude extracts were centrifuged at

Table 3 List of primers used in the real-time PCR analysis

Primers	Sequence (5′–3′)	Annealing temperature (°C)	Amplicon size (bp)
RPS (ribosomal protein small subunit 30S)	Sense: CGAAGTCAACCAGGAAACCAA	56	166
	Antisense: GTGCAAGAGACCGGACATACC		
TBP (TATA box binding protein)	Sense: ACCGGAGTCAAGAGCACACAC	56	175
	Antisense: CGGAATGCGCGTATACCAGT		
Rubisco (rbc S)	Sense: ACTCTGCTGGTGCTGTGCG	56	214
	Antisense: TGGGATTGGCGTCGTTCTT		
PRK	Sense: GAAGTTTGCTGTCTTTGCCTCT	56	139
	Antisense: GATGGGTGTCTGTCCCTCCT		
PGK	Sense: TGGTGGTGGCGACTCTGT	56	156
	Antisense: TACGCATTCCCGGCTTAC		
G6PDH	Sense: GCGAGAAATGGCACAAGG	56	180
	Antisense: GTTCATCGCAGTCGGGAGA		
6PGDH	Sense: GTTCACCGTTGCCGTTTG	56	143
	Antisense: CGACTTTCCGAGGCTTGCTG		

15,000*g* for 30 min at 4 °C, and the supernatants were used for proteins determination. The Coomassie Brilliant Blue G-250 assay was used for protein quantitation in the study [45].

Statistical analysis

All data are expressed as the mean ± standard deviation (SD) of three independent experiments. All statistical analyses were conducted using SPSS, and *t* test was used to identify data of any significance within the treatments at P value ≤ 0.05.

Abbreviations

OPPP: Oxidative pentose phosphate pathway; Rubisco: Ribulose-1, 5-bisphosphate carboxylase oxygenase; PGK: 3-phosphoglyceric phosphokinase; PRK: Phosphoribulokinase; G6PDH: Glucose-6-phosphate dehydrogenase; 6PGDH: 6-phosphogluconate dehydrogenase; RuBP: Ribulose-1,5-bisphosphate; PSII: Photosynthesis system II; DTT: DL-dithiothreitol; FW: Fresh weight; DCW: Dry cell weight; AFDW: Ash-free dry weight; TCA cycle: Tricarboxylic acid cycle; α-KGDH: α-ketoglutarate dehydrogenase; MDH: Malate dehydrogenase.

Competing interests

The authors declare that they have no competing interests.

Authors' contributions

SW, AH, and GW designed the experiments. SW and AH carried out the cultivation and analysis of lipid contents, enzyme activity, and mRNA expressions of *P. tricornutum*. BZ, LH, and PZ participated in the design of the primer used in the study. AL participated in the analysis of the photosynthetic performance of *P. tricornutum*. SW and GW drafted the manuscript. GW and AH revised the manuscript. GW conceived of the study. All authors read and approved the final manuscript.

Acknowledgements

This work was supported by International Science & Technology Cooperation Program of China (ISTCP, 2015DFG32160), Ministry of Science and Technology of the PRC fundamental research work (NO. 2012FY112900-01), the National Natural Science Foundation of China (41406169), the Science and Technology Strategic Pilot of the Chinese Academy of Sciences (XDA05030401), and Tianjin Natural Science foundation (12JCZDJC22200).

Author details

[1]Key Laboratory of Experimental Marine Biology, Institute of Oceanology, Chinese Academy of Sciences, Nanhai Road 7, Qingdao 266071, China. [2]College of Earth Sciences, University of Chinese Academy of Science, Beijing 100049, China.

Received: 26 June 2014 Accepted: 20 May 2015
Published online: 28 May 2015

References

1. Wu Y, Gao K, Riebesell U. CO_2-induced seawater acidification affects physiological performance of the marine diatom Phaeodactylum tricornutum. Biogeosciences. 2010;7:2915–23.
2. Gunderson CA, Wullschleger SD. Photosynthetic acclimation in trees to rising atmospheric CO2—a broader perspective. Photosynthesis Res. 1994;39:369–88.
3. Faria T, Wilkins D, Besford RT, Vaz M, Pereira JS, Chaves MM. Growth at elevated CO_2 leads to down-regulation of photosynthesis and altered response to high temperature in Quercus suber L. seedlings. J Exp Bot. 1996;47:1755–61.
4. Cheng SH, Moore BD, Seemann JR. Effects of short- and long-term elevated CO_2 on the expression of ribulose-1,5-bisphosphate carboxylase/oxygenase genes and carbohydrate accumulation in leaves of Arabidopsis thaliana (L.) Heynh. Plant Physiol. 1998;116:715–23.
5. Stitt M, Krapp A. The interaction between elevated carbon dioxide and nitrogen nutrition: the physiological and molecular background. Plant Cell Environ. 1999;22:583–621.
6. Bloom AJ, Smart DR, Nguyen DT, Searles PS. Nitrogen assimilation and growth of wheat under elevated carbon dioxide. Proc Natl Acad Sci U S A. 2002;99:1730–5.
7. Nakano Y, Miyatake K, Okuno H, Hamazaki K, Takenaka S, Honami N, et al. Growth of photosynthetic algae euglena in high CO_2 conditions and its photosynthetic characteristics. Acta Horticult (Wageningen). 1996;440:49–54.
8. Riebesell U, Wolfgladrow DA, Smetacek V. Carbon-dioxide limitation of marine phytoplankton growth rates. Nature. 1993;361:249–51.
9. Hein M, SandJensen K. CO_2 increases oceanic primary production. Nature. 1997;388:526–7.
10. Kim JM, Lee K, Shin K, Kang JH, Lee HW, Kim M, et al. The effect of seawater CO_2 concentration on growth of a natural phytoplankton assemblage in a controlled mesocosm experiment. Limnol Oceanogr. 2006;51:1629–36.
11. Tortell PD, Payne CD, Li YY, Trimborn S, Rost B, Smith WO, et al. CO_2 sensitivity of southern ocean phytoplankton. Geophys Res Lett. 2008;35.
12. Yongmanitchai W, Ward OP. Growth of and omega-3-fatty-acid production by Phaeodactylum tricornutum under different culture conditions. Appl Environ Microbiol. 1991;57:419–25.
13. Chiu S-Y, Kao C-Y, Tsai M-T, Ong S-C, Chen C-H, Lin C-S. Lipid accumulation and CO_2 utilization of Nannochloropsis oculata in response to CO_2 aeration. Bioresour Technol. 2009;100:833–8.
14. Tsuzuki M, Ohnuma E, Sato N, Takaku T, Kawaguchi A. Effects of CO_2 concentration during growth on fatty-acid composition in microalgae. Plant Physiol. 1990;93:851–6.
15. Yoo C, Jun SY, Lee JY, Ahn CY, Oh HM. Selection of microalgae for lipid production under high levels carbon dioxide. Bioresour Technol. 2010;101:S71–4.
16. Chisti Y. Biodiesel from microalgae. Biotechnol Adv. 2007;25:294–306.
17. Matsuda Y, Hara T, Colman B. Regulation of the induction of bicarbonate uptake by dissolved CO_2 in the marine diatom. Phaeodactylum tricornutum Plant Cell Environ. 2001;24:611–20.
18. Hyun B, Jang PG, Lee WJ, Shin K. Effects of increased CO_2 and temperature on the growth of four diatom species (Chaetoceros debilis, Chaetoceros didymus, Skeletonema costatum and Thalassiosira nordenskioeldii) in laboratory experiments. J Environ Sci Int. 2014;23:1003–12.
19. Schippers P, Lurling M, Scheffer M. Increase of atmospheric CO_2 promotes phytoplankton productivity. Ecol Lett. 2004;7:446–51.
20. Bermúdez M Jr (2010) Effect of CO_2 on elemental composition and fatty acids of diatoms and concomitant effects on copepods. Master thesis. Christian-Albrechts-Universität zu Kiel, Faculty of Mathematics and Natural Sciences; 2010.
21. Guschina IA, Harwood JL. Lipids and lipid metabolism in eukaryotic algae. Prog Lipid Res. 2006;45:160–86.
22. Harwood JL, Guschina IA. The versatility of algae and their lipid metabolism. Biochimie. 2009;91:679–84.
23. Allen JF. Photosynthesis of ATP— electrons, proton pumps, rotors, and poise. Cell. 2002;110:273–6.
24. Leninger A, Nelson DL, Cox MM. Principles of biochemistry. New York: Worth Publishers; 1993.
25. Li M, Ho PY, Yao SJ, Shimizu K. Effect of lpda gene knockout on the metabolism in Escherichia coli based on enzyme activities, intracellular metabolite concentrations and metabolic flux analysis by ^{13}C-labeling experiments. J Biotechnol. 2006;122:254–66.
26. Araujo SD, Garcia VMT. Growth and biochemical composition of the diatom Chaetoceros cf. wighamii brightwell under different temperature, salinity and carbon dioxide levels. I. Protein, carbohydrates and lipids. Aquaculture. 2005;246:405–12.
27. Gerard VA, Driscoll T. A spectrophotometric assay for rubisco activity: application to the kelp Laminaria saccharina and implications for radiometric assays. J Phycol. 1996;32:880–4.
28. Cescut J, Fillaudeau L, Molina-Jouve C, Uribelarrea J-L. Carbon accumulation in Rhodotorula glutinis induced by nitrogen limitation. Biotechnol Biofuels. 2014;7:164.
29. Li W, Gao KS, Beardall J. Interactive effects of ocean acidification and nitrogen-limitation on the diatom Phaeodactylum tricornutum. Plos One. 2012;7.
30. Hu Q, Sommerfeld M, Jarvis E, Ghirardi M, Posewitz M, Seibert M, et al. Microalgal triacylglycerols as feedstocks for biofuel production: perspectives and advances. Plant J. 2008;54:621–39.

31. Xiong W, Liu LX, Wu C, Yang C, Wu QY. ^{13}C-tracer and gas chromatography-mass spectrometry analyses reveal metabolic flux distribution in the oleaginous microalga Chlorella protothecoides. Plant Physiol. 2010;154:1001–11.
32. Recht L, Toepfer N, Batushansky A, Sikron N, Gibon Y, Fait A, et al. Metabolite profiling and integrative modeling reveal metabolic constraints for carbon partitioning under nitrogen starvation in the green algae Haematococcus pluvialis. J Biol Chem. 2014;289:30387–403.
33. Kletzien RF, Harris PKW, Foellmi LA. Glucose-6-phosphate-dehydrogenase—a housekeeping enzyme subject to tissue-specific regulation by hormones, nutrients, and oxidant stress. FASEB J. 1994;8:174–81.
34. Wu S, Zhang B, Huang A, Huan L, He L, Lin A, et al. Detection of intracellular neutral lipid content in the marine microalgae Prorocentrum micans and Phaeodactylum tricornutum using Nile red and BODIPY 505/515. J Appl Phycol. 2014;26:1659–68.
35. Guillard RR, Ryther JH. Studies of marine planktonic diatoms.1. Cyclotella nana Hustedt, and Detonula confervacea (Cleve) Gran. Can J Microbiol. 1962;8:229–39.
36. Lin AP, Wang GC, Yang F, Pan GH. Photosynthetic parameters of sexually different parts of Porphyra katadai var. hemiphylla (Bangiales, Rhodophyta) during dehydration and re-hydration. Planta. 2009;229:803–10.
37. Bligh E, Dyer WJ. A rapid method of total lipid extraction and purification. Can J Biochem Physiol. 1959;37:911–7.
38. Li W-q, Li Q, Liao Q-b, Chen Q-h. Effect of temperature on fatty acid composition of four species of marine microalgae. J Oceanogr Taiwan Strai. 2003;22:9–13.
39. Wang C, Fan XL, Wang GC, Niu JF, Zhou BC. Differential expression of Rubisco in sporophytes and gametophytes of some marine macroalgae. Plos One. 2011;6.
40. Rao IM, Terry N. Leaf phosphate status, photosynthesis, and carbon partitioning in sugar-beet. I. Changes in growth, gas-exchange, and calvin cycle enzymes. Plant Physiol. 1989;90:814–9.
41. Fahrendorf T, Ni WT, Shorrosh BS, Dixon RA. Stress responses in alfalfa (Medicago sativa L.). XIX. Transcriptional activation of oxidative pentose-phosphate pathway genes at the onset of the isoflavonoid phytoalexin response. Plant Mol Biol. 1995;28:885–900.
42. Peng L, Shimizu K. Global metabolic regulation analysis for Escherichia coli K12 based on protein expression by 2-dimensional electrophoresis and enzyme activity measurement. Appl Microbiol Biotechnol. 2003;61:163–78.
43. Jeffrey SW, Humphrey GF. New spectrophotometric equations for determining chlorophylls a, b, c1 and c2 in higher-plants, algae and natural phytoplankton. BPP. 1975;167:191–4.
44. Wang SB, Hu Q, Sommerfeld M, Chen F. An optimized protocol for isolation of soluble proteins from microalgae for two-dimensional gel electrophoresis analysis. J Appl Phycol. 2003;15:485–96.
45. Bradford MM. Rapid and sensitive method for quantitation of microgram quantities of protein utilizing principle of protein-dye binding. Anal Biochem. 1976;72:248–54.